

Structurally Simple Dipolar Organic Dyes Featuring 1,3-Cyclohexadiene Conjugated Unit for Dye-Sensitized Solar Cells

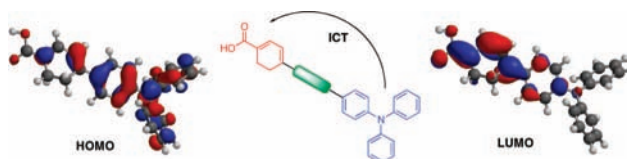
Kuan-Fu Chen,^{†,‡} Ying-Chan Hsu,[†] Qiongyou Wu,[†] Ming-Chang P. Yeh,^{*,‡} and Shih-Sheng Sun^{*,†}

*Institute of Chemistry, Academia Sinica, Nankang, Taipei 115, Taiwan, Republic of China
and Department of Chemistry, National Taiwan Normal University,
Taipei 11677, Taiwan, Republic of China*

sssun@chem.sinica.edu.tw; cheyeh@scc.ntnu.edu.tw

Received November 13, 2008

ABSTRACT



A series of structurally simple dipolar light-harvesting organic dyes featuring 1,3-cyclohexadiene in the aromatic π framework for dye-sensitized solar cells has been synthesized and characterized. The highest conversion efficiency of the DSSCs based on these dyes can reach up to 4.4%.

The effective harvesting solar energy and its conversion to electrical power has been a contemporary research topic for searching an energy alternative for the fossil fuel due to the increasing energy demands worldwide as well as the concerns of the global warming issue related to CO₂ emission from burning fossil fuel.¹ Dye-sensitized solar cells (DSSCs) based on organic and coordination complexes have received great attention among many research groups since the seminal report by Grätzel and co-workers.² Ru(II)-based complexes such as N3, N719, and the black dye have shown the best photoconversion efficiency up to 11% under AM 1.5 irradiation thus far.³ Although the efficiency of DSSCs based on organic dyes are generally lower than the cells based on Ru(II) dyes, the highest photoconversion efficiency of organic dye-sensitized solar cells has exceeded 9%.⁴ The advantages

of organic dyes over the Ru(II)-based metal complexes in DSSCs include the typically high molar absorption coefficients of organic dyes, a variety of specific functional groups of organic dyes available for tuning the absorption spectra coverage, the relative low costs of organic dye compared with those of ruthenium metal complexes, and essentially no limitation of resources.

Many kinds of organic dyes, such as coumarin-,⁵ cyanine-,⁶ hemicyanine-,⁷ triarylamine-,⁸ thiophene-,⁹ oligoene-,¹⁰ por-

(3) (a) Nazeeruddin, M. K.; Kay, A.; Rodicio, I.; Humphry-Baker, R.; Müller, E.; Liska, P.; Vlachopoulos, N.; Grätzel, M. *J. Am. Chem. Soc.* **1993**, *115*, 6382–6390. (b) Nazeeruddin, M. K.; Péchy, P.; Renouard, T.; Zakeeruddin, S. M.; Humphry-Baker, R.; Comte, P.; Liska, P.; Cevy, L.; Costa, E.; Shklover, V.; Spiccia, L.; Deacon, G. B.; Bignozzi, C. A.; Grätzel, M. *J. Am. Chem. Soc.* **2001**, *123*, 1613–1624. (c) Grätzel, M. *J. Photochem. Photobiol. A* **2004**, *164*, 3–14.

(4) (a) Ito, S.; Zakeeruddin, S. M.; Humphry-Baker, R.; Liska, P.; Charvet, R.; Comte, P.; Nazeeruddin, M. K.; Péchy, P.; Takata, M.; Miura, H.; Uchida, S.; Grätzel, M. *Adv. Mater.* **2006**, *18*, 1202–1205. (b) Horiuchi, T.; Miura, H.; Sumioka, K.; Uchida, S. *J. Am. Soc. Chem.* **2004**, *126*, 12218–12219. (c) Hwang, S.; Lee, J. H.; Park, C.; Lee, H.; Kim, C.; Park, C.; Lee, M.-H.; Lee, W.; Park, J.; Kim, K.; Park, N.-G.; Kim, C. *Chem. Commun.* **2007**, 488, 7–4889. (d) Ito, S.; Miura, H.; Uchida, S.; Takata, M.; Sumioka, K.; Liska, P.; Comte, P.; Péchy, P.; Grätzel, M. *Chem. Commun.* **2008**, 5194–5196.

[†] Academia Sinica.

[‡] National Taiwan Normal University.

(1) (a) Balzani, V.; Credi, A.; Venturi, M. *ChemSusChem* **2008**, *1*, 26–58. (b) Grätzel, M. *Nature* **2001**, *414*, 338–344. (c) Hagfeldt, A.; Grätzel, M. *Acc. Chem. Res.* **2000**, *33*, 269–277. (d) Robertson, N. *Angew. Chem., Int. Ed.* **2006**, *45*, 2338–2345.

(2) O'Regan, B.; Grätzel, M. *Nature* **1991**, *353*, 737–740.

phyrin,¹¹ and perylene-based¹² dyes have been exploited as photosensitizers for DSSCs. The structural composition of commonly seen organic dyes employed in the DSSCs typically consists of an electron donor, such as *para*-disubstituted aniline, and an electron acceptor, most notably cyanoacrylic acid, aiming to facilitate vectorial charge transfer upon light absorption, a π -conjugated spacer between the donor and acceptor to tune the spectral coverage and light harvesting efficiency, and an anchoring group to the TiO₂ surface integrated into the acceptor end.

In this study, we design a new class of organic sensitizers with a 1,3-cyclohexadiene conjugated unit as part of the spacer to link the electron donor and electron acceptor. The structures of these dyes are shown in Figure 1. A model

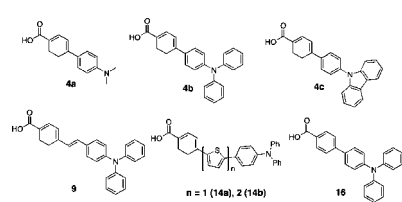


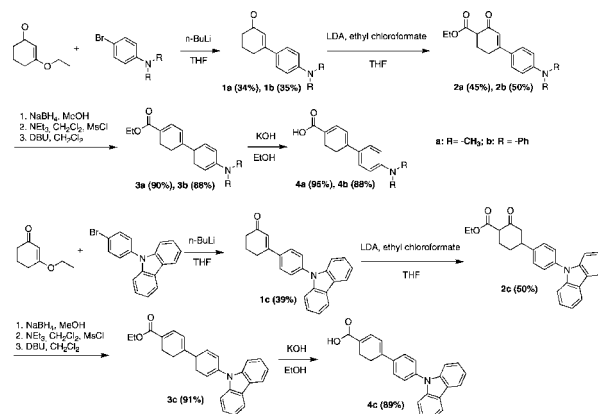
Figure 1. Structures of organic dyes.

compound **16** was also synthesized for assessing the role of 1,3-cyclohexadiene played in the photovoltaic efficiency. One obvious advantage of employing 1,3-cyclohexadiene unit in the framework of light-harvesting dyes is the essentially planar conformation in the structural skeleton which yields more dense packing of the dyes adsorbed on TiO₂ surface, not necessarily multilayer aggregation, and, therefore, increases the amounts of dye loading on the surface. The

integration of extended π -framework such as ethenyl, thiophene, and bithiophene unit would expect to further increase the spectrum coverage and better light harvesting efficiency. We have found that an appreciable photoconversion efficiency up to 4.4% can be achieved even with such structurally simple dyes.

The synthesis of dyes **4a–c** is summarized in Scheme 1, which followed the similar procedures. Lithiation with *n*-butyl lithium to 4-bromo-*N,N*-dimethylbenzenamine (4-

Scheme 1. Synthesis of Dipolar Dyes **4a–c**



bromo-*N,N*-diphenylbenzenamine or 4-bromo-*N*-carbazoylbenzenamine) followed by the nucleophilic addition–elimination reaction with 3-ethoxycyclohex-2-enone provided **1a–c**. Acylation of **1a–c** with ethyl chloroformate provided **2a–c**. The ester compounds **3a–c** were obtained by consecutive steps of reduction of cyclohexenone, methanesulfonylation, and elimination. Finally, the hydrolysis of the ester groups in compounds **3a–c** in aqueous KOH afforded the target dyes **4a–c**.

Scheme S1 (Supporting Information) describes the synthetic routes for dye **9**, which followed similar procedures to dyes **4a–c**. The key intermediate, compound **6**, was prepared by conventional Wittig reaction of 4-(diphenylamino)benzaldehyde with diethyl (3-oxocyclohex-1-en-1-yl)methylphosphonate. Dyes **14a** and **14b** were also synthesized in a similar manner by first synthesizing compounds **10a** and **10b** followed by palladium-catalyzed Suzuki coupling reactions to afford **11a** and **11b**. Subsequent acylation of **11a** and **11b** followed by reduction of cyclohexenone, methanesulfonylation, elimination, and hydrolysis afforded desired dyes **14a** and **14b** (Scheme S2, Supporting Information). Compound **16** was synthesized by palladium-catalyzed Suzuki coupling reaction of 4-(diphenylamino)phenylboronic acid with ethyl 4-bromobenzoate followed by hydrolysis in aqueous KOH (Scheme S3, Supporting Information). All dyes with 1,3-cyclohexadiene in the structure framework exhibit fairly good thermal stability. Except for **4c**, which starts to decompose at ~150 °C, the TGA data of other dyes showed no decomposition up to 200 °C. The photochemical stability of dyes **4b** and **14a** adsorbed on TiO₂ were also

- (5) (a) Hara, K.; Dan-oh, Y.; Kasada, C.; Ohga, Y.; Shinpo, A.; Suga, S.; Sayama, K.; Arakawa, H. *Langmuir* **2001**, *20*, 4205–4210. (b) Wang, Z.-S.; Cui, Y.; Dan-oh, Y.; Kasada, C.; Shinpo, A.; Hara, K. *J. Phys. Chem. C* **2007**, *111*, 7224–7230. (c) Wang, Z.-S.; Cui, Y.; Dan-oh, Y.; Kasada, C.; Shinpo, A.; Hara, K. *J. Phys. Chem. C* **2008**, *112*, 17011–17017.
- (6) Ehret, A.; Stuhl, L.; Spitler, M. T. *J. Phys. Chem. B* **2001**, *105*, 9960–9965.
- (7) (a) Stathatos, E.; Lianos, P. *Chem. Mater.* **2001**, *13*, 3888–3892. (b) Wang, Z.-S.; Li, F.-Y.; Huang, C.-H. *Chem. Commun.* **2000**, 2063–2064. (c) Yao, Q.-H.; Meng, F.-S.; Li, F.-Y.; Tian, H.; Huang, C.-H. *J. Mater. Chem.* **2003**, *13*, 1048–1053.
- (8) (a) Satoh, N.; Nakashima, T.; Yamamoto, K. *J. Am. Chem. Soc.* **2005**, *127*, 13030–13038. (b) Lu, J.; Xia, P. X.; Lo, P. K.; Tao, Y.; Wong, M. S. *Chem. Mater.* **2006**, *18*, 6194–6203. (c) Tsai, M.-S.; Hsu, Y.-C.; Lin, J. T.; Chen, H.-C.; Hsu, C.-P. *J. Phys. Chem. C* **2007**, *111*, 18785–18793. (d) Velusamy, M.; Thomas, K. R. J.; Lin, J. T.; Hsu, Y.-C.; Ho, K.-C. *Org. Lett.* **2005**, *7*, 1899–1902.
- (9) (a) Thomas, K. R. J.; Hsu, Y.-C.; Lin, J. T.; Lee, K.-M.; Ho, K.-C.; Lai, C.-H.; Cheng, Y.-M.; Chou, P.-T. *Chem. Mater.* **2008**, *20*, 1830–1840. (b) Liu, W.-H.; Wu, I.-C.; Lai, C.-H.; Chou, P.-T.; Li, Y.-T.; Chen, C.-L.; Hsu, Y.-Y.; Chi, Y. *Chem. Commun.* **2008**, 5152–5154.
- (10) Kitamura, T.; Ikeda, M.; Shigaki, K.; Inoue, T.; Anderson, N. A.; Ai, X.; Lian, T.; Yanagida, S. *Chem. Mater.* **2004**, *16*, 1806–1812.
- (11) (a) Campbell, W. M.; Jolley, K. W.; Wagner, P.; Wagner, K.; Walsh, P. J.; Gordon, K. C.; Schmidt-Mende, L.; Nazeeruddin, M. K.; Wang, Q.; Grätzel, M.; Officer, D. L. *J. Phys. Chem. C* **2007**, *111*, 11760–11762. (b) Eu, S.; Hayashi, S.; Umeyama, T.; Matano, Y.; Araki, Y.; Imahori, H. *J. Phys. Chem. C* **2008**, *112*, 4396–4405.
- (12) (a) Shibano, Y.; Umeyama, T.; Matano, Y.; Imahori, H. *Org. Lett.* **2007**, *9*, 1971–1974. (b) Edvinsson, T.; Li, C.; Pschirer, N.; Schöneboom, J.; Eickemeyer, F.; Sens, R.; Boschloo, G.; Herrmann, A.; Müllen, K.; Hagfeldt, A. *J. Phys. Chem. C* **2007**, *111*, 15137–15140.

tested under AM 1.5 irradiation for 3 h and showed no notable changes in the absorption spectra.

The absorption spectra of the dipolar dyes in acetonitrile solution are shown in Figure 2. The related photophysical

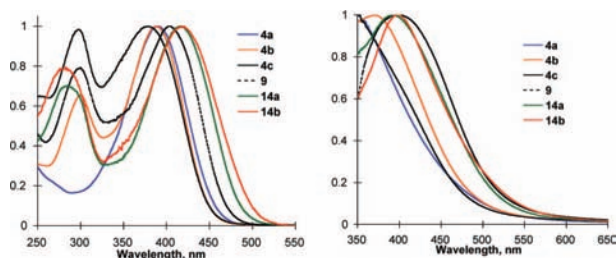


Figure 2. (Left) Normalized UV–vis absorption spectra of dyes in acetonitrile solution. (Right) Normalized absorption spectra of different dyes on 1.5 μm TiO_2 films.

data is summarized in Table 1. The general features of the absorption spectra consist of one broad band in the visible region and a less intense absorption band in the near UV

Table 1. Absorption and Fluorescence Properties^a

dye	λ_{max} , nm ($\epsilon \times 10^{-4}$, $\text{M}^{-1}\text{cm}^{-1}$)	λ_{em} , nm	dye loading, $10^{-6}\text{mol}/\text{cm}^2$
4a	391 (1.4)	481	1.0
4b	299 (2.3), 387 (1.5)	536	1.4
4c	298 (1.9), 379 (1.9)	447	1.0
9	300 (2.1), 404 (2.7)	528	1.5
14a	284 (1.6), 416 (2.3)	527	0.43
14b	279 (1.3), 417 (1.1)	542	0.38
16	350 (1.9)	501	0.97

^a Absorption and fluorescence spectra were measured in acetonitrile solution at 293 K. The fluorescence spectra were measured by excitation at the absorption maximum of the lowest energy band.

region, which correspond to an intramolecular charge transfer (ICT) transition and a locally excited $\pi-\pi^*$ transition, respectively. The broad absorption bands in these compounds suggest a good electronic delocalization throughout the whole molecular system. A systematic bathochromic shift in the absorption spectra with increasing conjugation was observed. Meanwhile, the spectra of **14a** and **14b** with thiophene moiety integrated into the conjugated structures are broader when compared to other four dyes due to the enhanced conjugation in these two molecules. DFT calculations at the B3LYP/6–31G* level of the theory support the directional charge transfer on excitation. The HOMO is primarily located on π -framework of triphenyl amine; whereas the electron density of LUMO is delocalized over the 1,3-cyclohexadienyl carboxylic acid moiety (Supporting Information). DFT calculations also indicated a smaller dihedral angle (28.0 and 33.5°) between the 1,3-cyclohexadienyl and phenyl moieties in **4b** when compared to the dihedral angle (34.6°) between

the two phenyl rings in model **16**, which suggests a more planar conformation in **4b**. The emission data in acetonitrile is also summarized in Table 1. The emission spectra exhibit significant solvatochromic shift in polar solvents indicative of an eminent ICT character.

The absorption spectra of the six dyes adsorbed on a transparent TiO_2 film are also shown in Figure 2. Compared to the corresponding spectra in CH_3CN solution, the spectral coverage become broader upon adsorption on TiO_2 but the absorption maxima shifted to higher energy when compared to that of in solution. Such blue shifts of the absorption spectra is attributed to either the formation of *H*-type aggregate¹³ or deprotonation of the carboxylic acid.^{9a} It should be noted here that the high absorption before 370 nm primarily belongs to TiO_2 and transparent FTO glass. The amount of dyes adsorbed on the TiO_2 surface was estimated from the difference in concentration of each solution before and after TiO_2 film immersion followed by rinsing with acetonitrile to ensure minimum physically adsorbed dyes left on the films. The data is also included in Table 1. It is pleased to see that the amount of dye adsorbed on TiO_2 film is extremely large and almost one to two orders higher than most of literature examples.¹⁴ The dye adsorption is directly related to the molecular size of dyes. The high dye-loading on the TiO_2 film indicates these structurally simple dyes with small molecular sizes formed a well organized monolayer on the TiO_2 surface, which is beneficial for the light harvesting efficiency.¹⁵

The oxidation potentials $E(\text{S}^+/\text{S})$ of the dyes were measured by cyclic voltammetry and the results are collected in Table 2. The oxidation potentials ranging from 0.87 to 1.50

Table 2. Electrochemical Data

dye	E_{0-0} , eV	$E(\text{S}^+/\text{S})$, V ^a	$E(\text{S}^+/\text{S}^*)$, V ^a	E_{gap} , V ^b
4a	2.84	0.87	−1.97	1.47
4b	2.81	1.04	−1.77	1.27
4c	2.81	1.50	−1.31	0.81
9	2.71	0.96	−1.75	1.25
14a	2.77	0.99	−1.78	1.28
14b	2.66	1.05	−1.61	1.11
16	3.01	1.22	−1.79	1.29

^a Potentials are vs NHE. ^b Energy gap between the excited-state oxidation potential and the TiO_2 conduction band edge.

V vs NHE are more positive than the redox the efficient thermodynamic driving force (0.37–1.10 V) for dye regeneration.

The excited-state oxidation potential $E(\text{S}^+/\text{S}^*)$ of these dyes can be obtained from the difference between the ground-

(13) Wang, Z.-S.; Hara, K.; Dan-oh, Y.; Kasada, C.; Shinpo, A.; Suga, S.; Arakawa, H.; Sugihara, H. *J. Phys. Chem. B* **2005**, *109*, 3907–3914.

(14) (a) Xu, W.; Peng, B.; Chen, J.; Liang, M.; Cai, F. *J. Phys. Chem. C* **2008**, *112*, 874–880. (b) Ning, Z.; Zhang, Q.; Wu, W.; Pei, H.; Liu, B.; Tian, H. *J. Org. Chem.* **2008**, *73*, 3791–3797. (c) Wang, Z.-S.; Koumura, N.; Cui, Y.; Takahashi, M.; Sekiguchi, H.; Mori, A.; Kubo, T.; Furube, A.; Hara, K. *Chem. Mater.* **2008**, *20*, 3993–4003. (d) Ooyama, Y.; Ishii, A.; Kagawa, Y.; Imae, I.; Harima, Y. *New J. Chem.* **2007**, *31*, 2076–2082.

(15) Mann, J. R.; Gannon, M. K.; Fitzgibbons, T. C.; Detty, M. R.; Watson, D. F. *J. Phys. Chem. C* **2008**, *112*, 13057–13061.

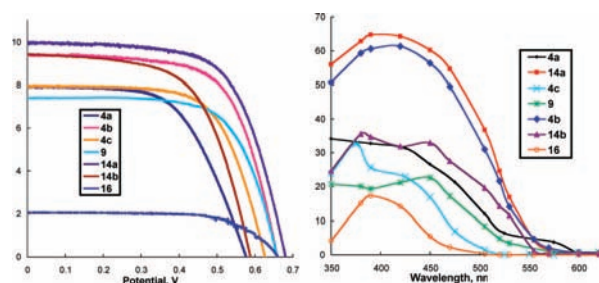


Figure 3. *J*–*V* curves (left) and IPCE plots (right) of the dyes.

state oxidation potential $E(S^+/S)$ and zero-zero excitation energy E_{0-0} ,¹⁷ which was estimated from the cross section of the normalized absorption and emission spectra. As shown in Table 2, the excited-state oxidation potentials of the six dyes are more negative than the potential of TiO₂ conduction band edge (–0.5 V vs NHE), which provides sufficient thermodynamic driving force (0.81–1.47 V) for electron injection.¹⁸

The device performance of solar cells based on the dyes with 1,3-cyclohexadiene linkage and the model **16** are summarized in Table 3. Figure 3 illustrates the *J*–*V* curves

Table 3. Photovoltaic Performance Parameters of the Dyes^a

dye	V_{OC} , mV	J_{SC} , mA/cm ²	<i>ff</i>	η , % ^b
4a	577	7.89	0.59	2.69 ± 0.20
4b	660	9.40	0.65	4.03 ± 0.01
4c	626	7.92	0.66	3.27 ± 0.33
9	660	7.39	0.64	3.33 ± 1.01
14a	682	9.92	0.65	4.40 ± 0.28
14b	585	9.42	0.60	3.31 ± 0.35
16	660	2.06	0.66	0.90 ± 0.01
N719	695	11.9	0.71	5.87 ± 0.02

^a Experiments were performed using TiO₂ photoelectrodes with approximately 16 μm thickness and 0.25 cm² working area on the FTO (15 Ω/sq.) substrates with electrolyte composed of 0.05 M I₂, 0.5 M LiI, and 0.5 M *tert*-butylpyridine in acetonitrile solution under AM 1.5 illumination.

^b Average of three measurements.

and action spectrum of incident photon-to-current conversion efficiency (IPCE) plots for the DSSCs based on the dyes studied in this work. The performance of the devices based on dyes **4b** and **14a** reach to 70% of the standard N719 dye. It should be pointed out here the reported η values in Table 3 were obtained without any of the additives typically used

such as deoxycholic acid nor optimizing the thickness of TiO₂ films for enhancing conversion efficiency. The DSSC based on model **16** with the 1,3-cyclohexadiene replaced by phenyl group shows only ~22% device efficiency of the one based on **4b**. With comparable V_{OC} and fill factor, the primary efficiency loss in **16** compared to **4b** is from the photocurrent, which is attributed to the more efficient charge transfer. The more planar 1,3-cyclohexadiene-phenyl conformation in **4b** is expected to yield more effective charge transfer to the anchoring carboxylate and perhaps better charge separation when compared to the biphenyl analogue **16**.

DSSCs based on dyes **4b** and **14a** produced maximum IPCE of 60–65% whereas those based on other dyes produced maximum IPCE below 40%. DSSCs based on dye **9** produced comparable V_{OC} and fill factor to dyes **4b** and **14a** but considerable lower photocurrent and, thus, IPCE performance. The IPCE is derived from the product of light harvesting efficiency (LHE) of the dye-loaded film, the quantum yield of the electron injection (CIE), and the efficiency of collecting the injected electron (CCE).^{3a,14c} Since the absorbance is in the range of 0.6–1.3 for the dye-loaded 1.5 μm TiO₂ film, the LHE would be close to unity for dye-loaded 16 μm TiO₂ films. Electron injection yield would be also comparable between dyes **4b**, **14a**, and **9** considering the similar driving force for electron injection. Therefore, the reduced photocurrent in DSSC based on **9**, which exhibited highest dye loading on TiO₂ surface, is attributed to the serious charge recombination due to the significant dye aggregates formed on the TiO₂ surface which may block the infusion of redox mediator into the nanoporous TiO₂.^{14c} The same effect also influenced the resulting V_{OC} values. The thicker dye aggregates would block the I₃[–] approaching the TiO₂ surface and reduced the probability of back electron transfer from injected electron to reduce the I₃[–]. As shown in Tables 1 and 3, the amount of dye adsorbed on TiO₂ surface qualitatively correlated with the V_{OC} with the lowest V_{OC} generated from DSSC based on least adsorbed **14b**.

In summary, a series of structurally simple dipolar organic dyes with 1,3-cyclohexadiene integrated in the π -conjugated backbone has been synthesized in high yields. DSSCs based on these dyes have shown appreciable phototo-electrical energy conversion efficiency with the highest one up to 4.4%. Further structural optimization with broad spectral coverage and enhancing directionality of charge transfer in the excited-state is expected to produce more efficient photosensitizers. Our work toward these directions are underway.

Acknowledgment. We thank the National Science Council in Taiwan, Academia Sinica, and National Taiwan Normal University for support of this research.

Supporting Information Available: Synthesis, experimental procedures, characterization data, molecular orbital plots, and TGA plots. This material is available free of charge via the Internet at <http://pubs.acs.org>.

OL802630X

(16) Koumura, N.; Wang, Z.-S.; Mori, S.; Miyashita, M.; Suzuki, E.; Hara, K. *J. Am. Chem. Soc.* **2006**, *128*, 14256–14257.

(17) Klein, C.; Nazeeruddin, M. K.; Liska, P.; Censo, D.; Hirata, N.; Palomares, E.; Durrant, J. R.; Grätzel, M. *Inorg. Chem.* **2005**, *44*, 178–180.

(18) (a) Hara, K.; Sato, T.; Katoh, R.; Furube, A.; Ohga, Y.; Shinpo, A.; Suga, S.; Sayama, K.; Sugihara, H.; Arakawa, H. *J. Phys. Chem. B* **2003**, *107*, 597–606. (b) Hagfeldt, A.; Grätzel, M. *Chem. Rev.* **1995**, *95*, 49–68.